

Square Planar Co-ordination of the 12-Membered Macrocyclic Tetra-amine Ligand 1,4,7,10-Tetra-azacyclododecane-2,6-dione

By **Mutsuo Kodama**, Department of Chemistry, College of General Education, Hirosaki University, Bunkyo, Hirosaki 036, Japan

Eiichi Kimura,* Department of Medicinal Chemistry, Hiroshima University School of Medicine, Kasumi, Hiroshima 734, Japan

A novel example of square-planar N_4 co-ordination of a 12-membered macrocycle has been found with the title compound, L^5 . Rigid planarity caused by the dissociation of two protons from the amide groups at pH *ca.* 8 stabilizes the 1 : 1 complex $[M(H_2L)]$, with $M = Cu^{2+}$ and Ni^{2+} , as shown by pH-metric titrations. The conceivable bond strain around Cu^{2+} is manifested in the visible spectrum exhibiting an unusual blue shift and also in the cumulative formation constant $K_{CuH_2L} \{ = [Cu(H_2L)][H^+]^2/[Cu^{2+}][L] \}$ which is much smaller than the reported values for the square-planar complexes of 13–15-membered homologous macrocycles, L^6-L^8 , or glycyglycylglycine, L^{11} . The advantages of the planar ligand field and the small cavity size are reflected in the ready attainment of a d^9 Cu^{2+} complex as demonstrated by the extremely low electrode potential E° measured using cyclic voltammetry. In contrast, Ni^{2+} with a smaller cation size seems to fit more easily in the 12-membered cavity. The K_{NiH_2L} value is comparable to that for L^{11} . The yellow visible spectrum is indicative of low-spin square-planar complex geometry.

THE feasibility of square-planar co-ordination for the quadridentate 12-membered macrocycle 1,4,7,10-tetra-azacyclododecane, L^1 , had been inferred,¹ although its existence had long remained unverified. Very recently, Fabbri reported² that the blue coloured (high-spin) aqueous solution of octahedral *cis*- $[NiL^1]^{2+}$ is partially convertible into a yellow coloured low-spin planar species under special conditions. Normally, however, it is more than 99% in the high-spin form.³ The copper complex of L^1 is reported to adopt a square-pyramidal structure.³

Herein we describe a new 12-membered tetra-amine ligand containing two amide groups, L^5 , designed to enforce a square-planar configuration on interaction with divalent metal ions. The molecular structure mimics tripeptides such as glycyglycylglycine, L^{11} (refs. 4 and 5), and is an extension of the 13–15-membered dioxotetra-amine series, L^6-L^8 . These potential quadridentate macrocycles were all shown to form square-planar N_4 (including two imide nitrogens) complexes $[M(H_2L)]$ with M^{2+} ($=Cu^{2+}$ and Co^{2+}) as a result of double deprotonation of the amides. The present potentiometric measurements on L^5 with Cu^{2+} and Ni^{2+} have also demonstrated the dissociation of the two protons from the two amide groups to form the $[M(H_2L)]$ complex. Square-planar complex geometry with Ni^{2+} is strongly indicated spectrophotometrically. A parallel study of the complexes of L^6-L^9 with Ni^{2+} has lent support to the assignment of planar co-ordination in $[Ni(H_2L)]$ complexes. As an illustration of the small cavity size and the rigid planarity of L^5 , we have examined, by cyclic voltammetry, the electrode potentials E° needed to attain uncommon trivalent oxidation states of Cu and Ni encircled by the doubly deprotonated L^5 .

EXPERIMENTAL

The 12-membered macrocycle L^5 was first synthesized by Tabushi *et al.*⁹ as an intermediate to L^1 . The procedure involves reaction of 1,5-diamino-3-azapentane with diethyl

iminodiacetate in refluxing ethanol for 72 h, followed by chromatographic purification on silica gel [eluant, $CHCl_3$ -MeOH (2 : 1)]. The compound (hygroscopic) was recrystallized carefully from ethanol, m.p. 160 °C (lit.,⁹ 163–165 °C). The proton n.m.r. spectrum agreed with that of the reference.⁹ Mixed protonation constants K_i determined potentiometrically were 7.60 (7.40) and 4.40 (4.20) at

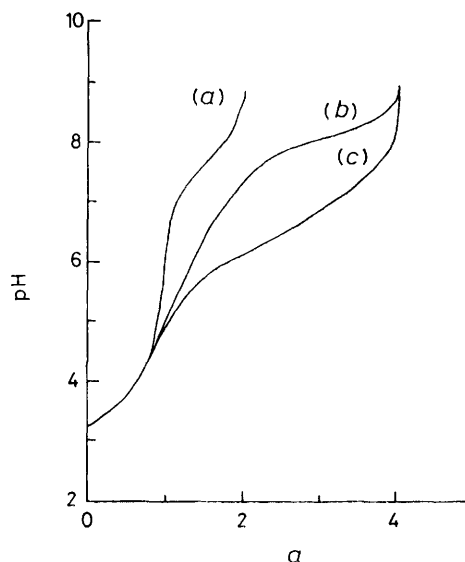
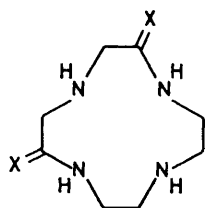
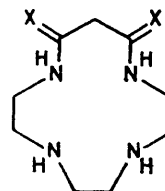


FIGURE 1 Potentiometric titration equilibrium curves of $L^5 \cdot 2HClO_4$ (2×10^{-3} mol dm^{-3}) (a) on its own, (b) with Ni^{2+} , and (c) with Cu^{2+} ($[Ni^{2+}] = [Cu^{2+}] = 2 \times 10^{-3}$ mol dm^{-3})

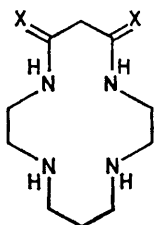
I 0.2 mol dm^{-3} and 25 °C (35 °C). Other dioxotetra amines were prepared as before.⁶ The salts $Cu[NO_3]_2$ and $NiCl_2$ were analytical grade chemicals and their solutions were standardized by titration with ethylenediaminetetraacetate (edta) by the method of Schwarzenbach.¹⁰ Potentiometric titrations (Figure 1) were performed in the same way as those for the Cu^{2+} - L^6-L^9 mixtures (equimolar concentrations of $L^5 \cdot 2HClO_4$ and metal ions).⁶ In the case of Ni^{2+} - L^5-L^9 each titration point required 10–15 min to



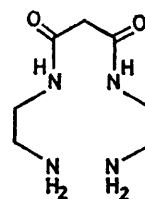
$L^1, X = H_2$
 1,4,7,10-Tetra-azacyclododecane
 $L^5, X = O$
 1,4,7,10-Tetra-azacyclododecane-2,6-dione



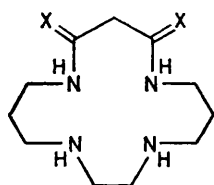
$L^2, X = H_2$
 1,4,7,10-Tetra-azacyclotridecane
 $L^6, X = O$
 1,4,7,10-Tetra-azacyclotridecane-11,13-dione



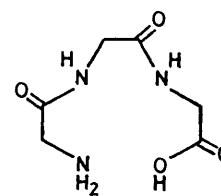
$L^3, X = H_2$
 1,4,8,11-Tetra-azacyclotetradecane
 $L^7, X = O$
 1,4,8,11-Tetra-azacyclotetradecane-12,14-dione



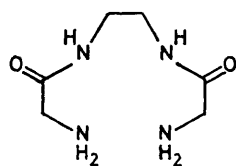
L^9
 1,9-Diamino-3,7-diaza-nonane-4,6-dione



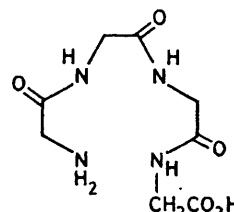
$L^4, X = H_2$
 1,4,8,12-Tetra-azacyclopentadecane
 $L^8, X = O$
 1,4,8,12-Tetra-azacyclopentadecane-9,11-dione



L^{11}
 Glycylglycylglycine



L^{10}
 1,8-Diamino-3,6-diaza-octane-2,7-dione



L^{12}
 Glycylglycylglycylglycine

reach equilibrium at 35 °C (at 25 °C the equilibrating time is much longer). Cyclic voltammetry was performed at 25 °C for both the copper and nickel systems with a three-electrode system consisting of a glassy carbon working electrode, a platinum-wire auxiliary electrode, and a saturated calomel reference electrode (s.c.e.). Voltammograms were generated using a solid-state potentiostat and a potential scanner constructed in this laboratory, following the design of Itabashi and Oikawa,¹¹ and recorded on a Rika Denki RW-11 X-Y recorder. A working electrode was constructed from a 3-mm glassy carbon rod (Grade GC-20, Tokai Electrode Company). The visible spectra were obtained with a Hitachi 200-10 spectrophotometer.

Determination of E^\ominus Values.—Electrochemical analyses by voltammetry were used to determine the electrode potentials, E^\ominus , of a series of metal(II)-macrocycle complexes in a similar fashion to those applied on peptide complexes of Cu^{2+} ¹² and Ni^{2+} .¹³ Figure 2 shows a typical current-

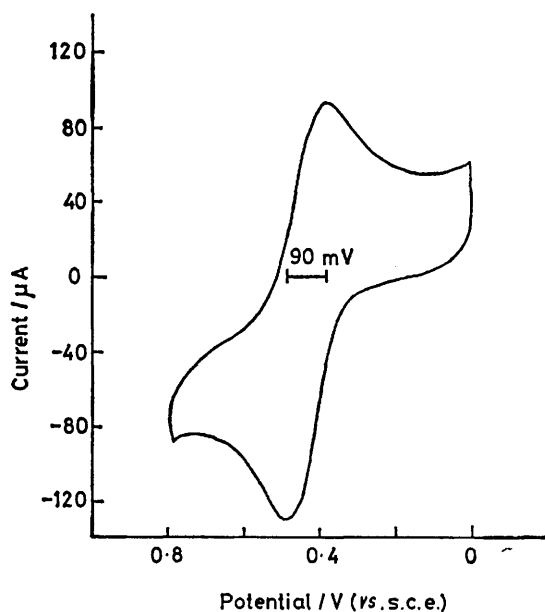


FIGURE 2 Cyclic voltammogram of $[\text{Cu}(\text{H}_2\text{L})]_9$ (10^{-3} mol dm^{-3}) where $\text{L} = \text{L}^5$ in aqueous solution at a glassy carbon electrode. $E^\ominus = 0.42$ V vs. s.c.e., pH = 9.6, $I = 0.5$ mol dm^{-3} ($\text{Na}_2[\text{SO}_4]$)

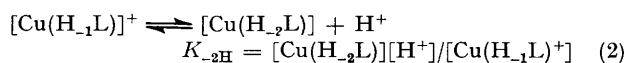
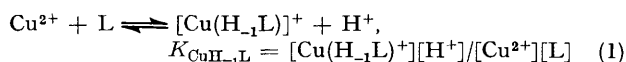
voltage response obtained in $\text{Na}_2[\text{SO}_4]$ (0.5 mol dm^{-3}) solution at 25 °C and a scan rate of 100 mV s^{-1} for the copper(II)- L^5 complex (10^{-3} mol dm^{-3}) (pH = 9.6). The initial solution contains only the divalent complex which generates the oxidation wave, while the oxidized trivalent complex formed in the anodic scan generates the reduction wave. This current-voltage response curve is representative of all the copper(II) and nickel(II) complexes studied (see Table). The electrode potentials were obtained from an average of three measurements and have a reproducibility of ± 3 mV. All the E^\ominus values are given in terms of standard electrode potentials (V) vs. s.c.e.

The separation of anodic and cathodic peaks, ΔE , was 70–90 mV in all but a few cases and peak height ratios were near unity. Slight variations (± 3 mV) of peak potential separation with different scan rates (from 20 to 300 mV s^{-1}) were also observed. Furthermore, both peak heights were proportional to the square root of scan rate, $V^{1/2}$. These features are indicative of quasi-reversible (one-

electron) electrochemical behaviour, and therefore the midpoint between two peaks should be a reasonable estimate of the electrode potential corresponding to the polarographic half-wave potential, $E_{1/2}$.¹⁴ In all cases the midpoint between the two peak potentials was found to be independent of the solution pH: with Ni^{2+} and L^5 (pH 9.5–10.5), L^6 (7.7–10.0), L^7 (7.0–10.5), L^8 (8.5–11.0); with Cu^{2+} and L^5 (9.3–10.2), L^6 (6.2–10), L^7 (5.8–10.5), L^8 (7.7–10.5), L^9 (9.3–10.5). The midpoint was also independent of the concentrations of complexes (5×10^{-1} – 4×10^{-3} mol dm^{-3}) and uncomplexed ligands (5×10^{-2} – 5×10^{-3} mol dm^{-3}).

RESULTS

Copper(II)- L^5 System.—*pH-Metric titrations.* The pH titration curve under an atmosphere of nitrogen at 25 °C showed complexation to occur above $a = 1$ and two breaks, one (very slight) at $a = 3$ and the other at $a = 4$, where a represents the number of moles of $\text{Na}[\text{OH}]$ added per mole of ligand (as the 2HClO_4 salt) present in solution. The complexation equilibria in equations (1) and (2) were presumed.



The $K_{\text{CuH}_{-1}\text{L}}$ value was determined in an analogous way to that described for L^6 – L^8 complexation $\{\text{M}^{2+} + \text{L} \rightleftharpoons [\text{M}(\text{H}_{-2}\text{L})] + 2\text{H}^+, K_{\text{CuH}_{-2}\text{L}}\}$.⁶ Briefly, taking into account the existence of $[\text{Cu}(\text{OH})]^+$ $\{K_{\text{OH}} = [\text{Cu}(\text{OH})^+]/[\text{Cu}^{2+}][\text{OH}^-] = 10^{6.1}\}$,^{15,*} the conditional constant K for (1) is

$$K = \frac{K_{\text{MH}_{-1}\text{L}}/(\alpha_{\text{H}})_{\text{L}}(1 + K_{\text{OH}}[\text{OH}^-])}{[\text{MH}_{-1}\text{L}^+][\text{H}^+]/[\text{M}^{2+}]_{\text{ap}}[\text{L}]_{\text{F}}} \quad (3)$$

expressed as in equation (3).† Appropriate combination of the terms (4)–(8) (for their definition and derivation, see ref. 6) and substitution into (3) leads to equation (9) at $c_{\text{L}} = c_{\text{M}}$.

$$\alpha = ac_{\text{L}} + [\text{H}^+] = 2[\text{L}] + [\text{HL}^+] + 3[\text{M}(\text{H}_{-1}\text{L})^+] + [\text{M}(\text{OH})^+] \quad (4)$$

$$\beta = 2 + [\text{H}^+]K_1 \quad (5)$$

$$(\alpha_{\text{H}})_{\text{L}} = \frac{[\text{L}]_{\text{F}}}{[\text{L}]} = 1 + [\text{H}^+]K_1 + [\text{H}^+]^2K_1K_2 \quad (6)$$

$$R = \frac{K_{\text{OH}}[\text{OH}^-]}{(1 + K_{\text{OH}}[\text{OH}^-])} \quad (7)$$

$$[\text{M}^{2+}]_{\text{ap}} = [\text{M}^{2+}] + [\text{M}(\text{OH})^+] \quad (8)$$

$$\frac{K_{\text{MH}_{-1}\text{L}}}{1 + K_{\text{OH}}[\text{OH}^-]} = \frac{\{(\alpha_{\text{H}})_{\text{L}}(\alpha - Rc_{\text{L}}) - \beta_{\text{H}}c_{\text{L}}\}\{(3 - R)(\alpha_{\text{H}})_{\text{L}} - \beta_{\text{H}}\}[\text{H}^+]}{(3c_{\text{L}} - \alpha)^2(\alpha_{\text{H}})_{\text{L}}} \quad (9)$$

For the titration data at $1 < a < 3$ (where *ca.* $5 < \text{pH} < 7$), the plots of the numerator vs. denominator of the right-hand side of equation (9) were linear and passed through the origin. The $K_{\text{MH}_{-1}\text{L}}$ value was calculated from the gradient.

For the titration region $3 < a < 4$ (where *ca.* $7 < \text{pH} < 8$), substitution of equations (10)–(12) into equation (2) yields equation (13). Plots of $(a - 3)/(4 - a)$ against

$$\alpha = ac_{\text{L}} + [\text{H}^+] \approx ac_{\text{L}} \quad (10)$$

* The value cited is corrected for $I = 0.2$ mol dm^{-3} .
† $[\text{M}^{2+}]_{\text{ap}}$ = Apparent concentration of M^{2+} .

$[\text{H}^+]^{-1}$ (hydrogen-ion concentrations were read directly from pH) were linear and passed through the origin.

$$[\text{M}(\text{H}_2\text{L})] = (a - 3)c_L \quad (11)$$

$$c_L = [\text{M}(\text{H}_1\text{L})^+] + [\text{M}(\text{H}_2\text{L})] \quad (12)$$

$$K_{-2\text{H}} = \{(a - 3)/(4 - a)\}[\text{H}^+] \quad (13)$$

Visible spectra. The absorption spectra of Cu^{2+} - L^5 solutions are shown in Figure 3. Before addition of base, little complex formation takes place (curve 1). As the concentration of base added is increased, the band maximum shifts to shorter wavelengths and increases in intensity (curves 2–4). Curve 4 (λ_{max} , 650 nm) is almost entirely

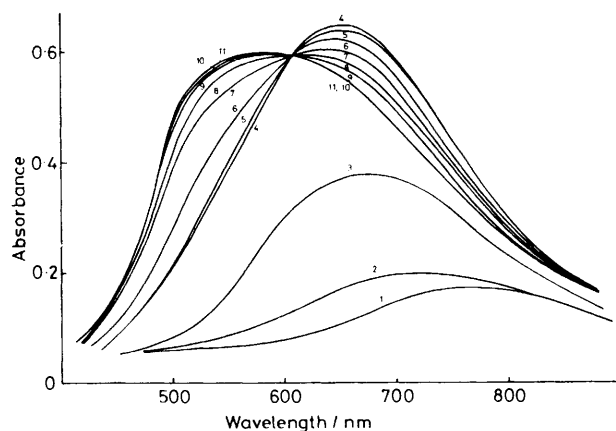
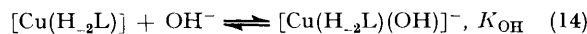


FIGURE 3 Visible absorption spectra of copper(II)- L^5 solutions. All solutions are 4×10^{-3} mol dm^{-3} in Cu^{2+} and in L^5 , and 0.2 mol dm^{-3} in $\text{Na}[\text{ClO}_4]$. The solution pH values are (1) 4.1, (2) 5.3, (3) 6.0, (4) 6.5, (5) 6.9, (6) 7.4, (7) 7.9, (8) 8.5, (9) 9.3, (10) 11.6, and (11) 12.5

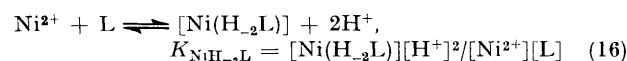
(95%) due to the species $[\text{Cu}(\text{H}_1\text{L})]^+$ [the remaining 5% due to $\text{Cu}^{2+}(\text{aq.})$ based on the equilibrium constants determined potentiometrically]. Curves 4–9 give an isosbestic point (at 612 nm) which confirms the potentiometric finding that only two species, $[\text{Cu}(\text{H}_1\text{L})]^+$ and $[\text{Cu}(\text{H}_2\text{L})]$, are present in the region from $a = 3$ to 4. At pH 9.5 (curve 9), 98% of the copper is calculated to be present as $[\text{Cu}(\text{H}_2\text{L})]$.

The spectra (see absorptions at ca. 650 nm) at $9.5 < \text{pH} < 11.6$ suggest an acid-base equilibrium yielding a hydroxo-complex, equation (14). The equilibrium constant K_{OH}



(4.5×10^3) was obtained using the limiting absorbances at 660 nm for $[\text{Cu}(\text{H}_2\text{L})]$ (0.76) and $[\text{Cu}(\text{H}_2\text{L})(\text{OH})]^-$ (0.55), both at 4×10^{-3} mol dm^{-3} . At pH 11.6, the $[\text{Cu}(\text{H}_2\text{L})(\text{OH})]^-$ species constitutes 95% of all the copper species.

Nickel(II)-Dioxotetra-amine System.—The titration curve for L^5 (see Figure 1) at $c_L = c_M$ and 35 °C indicated interaction with Ni^{2+} above $a = 1$. The equilibria (15) and (16) explain the mode of L^5 complexation with Ni^{2+} .



The titration data at $1 < a < 2$ (ca. $4.5 < \text{pH} < \text{ca. } 7.5$) fit equation (17) which is immediately derived from

$$K_{\text{NiL}} = \frac{\{\alpha(\alpha_{\text{H}})_L - \beta_{\text{H}}c_L\}\{2(\alpha_{\text{H}})_L - \beta_{\text{H}}\}}{(2c_L - \alpha)^2(\alpha_{\text{H}})_L} \quad (17)$$

equation (9) by placing $R = 0$ (justifiable in view of $K_{\text{OH}} = 10^{4.5}$ mol dm^{-3})¹² and treating L as a diacid base instead of the triacid base.

At $2 < a < 3.6$ ($7.5 < \text{pH} < 8.5$), the data are in accord with equation (18), which is immediately borne out by treating L as a tetra-acid base instead of the triacid base of equation (9). A linear relation was found between the numerator and denominator of the right-hand side.

$$\frac{K_{\text{Ni}(\text{H}_2\text{L})}}{1 + K_{\text{OH}}[\text{OH}^-]} = \frac{\{(\alpha_{\text{H}})_L(\alpha - Rc_L) - \beta_{\text{H}}c_L\}\{(4 - R)(\alpha_{\text{H}})_L - \beta_{\text{H}}\}[\text{H}^+]^2}{(4c_L - \alpha)^2(\alpha_{\text{H}})_L} \quad (18)$$

For the L^6 (complexation occurs at pH 6.1–7), L^7 (pH 6–6.3), L^8 (pH 7.3–7.6), and L^9 (pH 7.8–8) systems, all the titration data for complexation obeyed equation (18) to establish equilibrium (16). All the results are summarized in the Table, along with previously reported relevant values.

Visible spectra of the Ni^{2+} - L^5 system. The absorption spectra are shown in Figure 4. As the concentration of base is increased, the bands due to $\text{Ni}^{2+}(\text{aq.})$ (395 and 690 nm, curve 1) shift slightly toward shorter wavelengths, 380 and 650 nm, with a slight increase in intensity. At pH 6.7, 30% of the nickel species should exist as $[\text{NiL}]^{2+}$ according to the potentiometric interpretation. The spectra thus indicate the $[\text{NiL}]^{2+}$ complex to be octahedral. As the concentration of base is further increased beyond $a = 2$, i.e. $7.5 < \text{pH} < 10$, curves 3–8, a new band at 465 nm

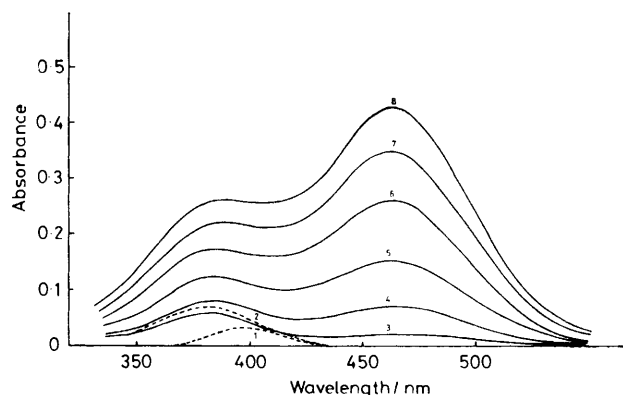
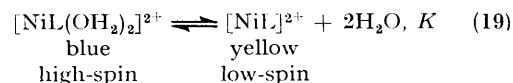


FIGURE 4 Absorption spectra of nickel(II)- L^5 solutions. All solutions are 5×10^{-3} mol dm^{-3} in Ni^{2+} and L^5 , and 0.2 mol dm^{-3} in $\text{Na}[\text{ClO}_4]$. The solution pH values are (1) 4.0, (2) 6.0, (3) 7.6, (4) 7.9, (5) 8.2, (6) 8.4, (7) 8.7, and (8) 9.0, 9.5, and 10.3

increases in intensity along with the band at 380 nm. At pH 7.9, curve 4, $[\text{NiL}]^{2+}$ (50%) and $[\text{Ni}(\text{H}_2\text{L})]$ (50%) are coexistent. At pH > 8.9 , curve 8, $[\text{Ni}(\text{H}_2\text{L})]$ is the sole nickel species. For the spectra above pH 9 we assign the absorption maximum at 465 nm to the low-spin, square-planar complex and the one at 380 nm to the high-spin, octahedral complex.

For the nickel complexes of the dioxo-free ligands L^1 – L^4 , it is well known that the blue-to-yellow equilibrium (19) exists and that it is shifted to the right by increasing



ionic strength and temperature.^{3,3,16,17} With the L^5 system, likewise, increasing temperature and/or $\text{Na}[\text{ClO}_4]$

concentration resulted in an increase in the intensity of the band at 465 nm, with a simultaneous decrease in the intensity of the band at 380 nm. The limiting spectrum for the yellow species was obtained at 50 °C and I 8 mol dm⁻³, where the band at 380 nm disappeared and the temperature increase did not cause any further increase in the intensity of the band at 465 nm. The equilibrium constant K for the L⁵ complex was investigated at I 0.2 mol dm⁻³ over the temperature range 2.5–50 °C. The obtained log K values were 0.24 (2.4), 0.44 (10.0), 0.74 (25.0), 1.10 (41.0), and 1.41 (50.4 °C). Thus, one may conclude that the L⁵ complex

The yellow absorption bands at 410–465 nm (see Table) for all the dioxotetra-amines indicate more or less coplanar arrangement of the four nitrogen donors. Similar absorption band ranges have been reported for the low-spin square-planar complexes of macrocyclic dioxo-free tetra-amines: L¹ 430 nm,² L³ 444 nm,¹⁶ isomeric L³ 463 nm,¹⁹ or L⁴ 466 nm.^{2,*} The energy of the band in this region has been used as a measure of the Ni–N interactions in the square-planar L¹–L⁴ complexes. Among the complexes of the dioxo-ligands,

Properties of metal–macrocycle complexes at I 0.2 mol dm⁻³ and 25 °C (Cu²⁺) or 35 °C (Ni²⁺) unless otherwise noted

Metal ion	Ligand	K_{MH_2L} ^a /mol dm ⁻³	$\lambda_{max.}/nm$ ^b ($\epsilon/dm^3 mol^{-1} cm^{-1}$)	E^\ominus c, V vs. s.c.e.	Δ ^d /mV	Notes	
Copper(II)	L ⁵ (pH 9.60)	$6.8 \pm 0.5 \times 10^{-10}$	ca. 620 (150)	0.42 ₀	90	$K_{CuH_2L} = 3.6 \times 10^{-2}$	
	L ⁶ (pH 9.50)	$6.3 \times 10^{-3} e$	520 (100) ^e	0.56 ₀	90		
	L ⁷ (pH 9.80)	1.0×10^e	505 (ca. 100) ^e	0.64 ₀	80		
	L ⁸ (pH 9.00)	$3.2 \times 10^{-6} e$	520 (100) ^e	0.69 ₀	100		
	L ⁹ (pH 9.30)	$8.4 \times 10^{-6} e$	515 (100) ^e	0.70 ₀	75		
	L ¹⁰ f	$10^{-6.3}$	518	0.77 ^g			
	L ¹¹ (pH 7.7) h	$10^{-6.5}$	555 (100)	0.67 ⁱ	78	$K_{CuH_2L} = 10^{9.1}$ Triply deprotonated species	
	L ¹² (pH 9.5) h		515	0.38 ⁱ	85		
	Nickel(II)	L ⁵ (pH 9.50)	$1.1 \pm 0.1 \times 10^{-13}$	465 (100)	0.62 ₀	100	$K_{NiL} = 6.6 \times 10^3 dm^3 mol^{-1}$
		L ⁶ (pH 9.50)	$9.0 \pm 0.9 \times 10^{-7}$	412 (110)	0.90 ₀	80	
		L ⁷ (pH 8.30)	$7.0 \pm 0.8 \times 10^{-6}$	460 (100)	0.80 ₀	80	
		L ⁸ (pH 8.80)	$1.2 \pm 0.1 \times 10^{-9}$	450 (100)	0.62 ₁	100	
L ⁹		$9.9 \pm 1.0 \times 10^{-13}$	450 (80)	Irreversible Wave			
L ¹⁰ f		$10^{-10.7}$	414				
L ¹¹ (pH 9.6) j		$10^{-12.8}$	430	0.60 ^k	81	$K_{NiL} = 10^{5.38} dm^3 mol^{-1}$ $K_{NiL} = 10^{3.7} dm^3 mol^{-1}$ Triply deprotonated species	
L ¹² (pH 9.6) j			412	0.54 ^k	98		

^a Cumulative formation constants (with confidence limits) of doubly deprotonated metal(II) complexes. See equation (16).
^b Visible absorption maximum of the doubly (or triply) deprotonated metal(II) complex. ^c ± 3 mV. Determined by cyclic voltammetry at 100 mV s⁻¹ with a glassy carbon electrode at 25 °C. The pH values of ML solutions used in the electrochemical study are given with the ligands. ^d Peak potential separation indicating reversibility of the electrode reaction ($\Delta = 59.5$ mV for a one-electron couple which is completely reversible electrochemically). ^e Ref. 6. ^f Ref. 18. ^g P. Stevens, J. M. Waldeck, J. Strohl, and R. Nakon, *J. Am. Chem. Soc.*, 1978, **100**, 3632. ^h M. K. Kim and A. E. Martell, *J. Am. Chem. Soc.*, 1966, **88**, 914. ⁱ Ref. 12. Corrected from V vs. n.h.e. ^j M. K. Kim and A. E. Martell, *J. Am. Chem. Soc.*, 1967, **89**, 5138. ^k Ref. 13.

[Ni(H₂L)] is 85% in the square-planar form and 15% in the octahedral form at 25 °C.

For other macrocyclic dioxo-systems L⁶–L⁸, only the 410–460 nm absorption occurs. The temperature increase caused a slight increase in the band intensity. Accordingly, we determined the equilibrium constants K of equation (19). The molar absorptivities of the planar complexes needed for the calculation were taken from the limiting spectra at 50 °C and I 8 mol dm⁻³. The log K values are 1.7 (L⁶), 1.6 (L⁷), and 2.5 (L⁸) at 25 °C and I 0.2 mol dm⁻³ (Na[ClO₄]).

DISCUSSION

Nickel(II)–Dioxotetra-amine Complexation.—The pH-metric titration results show the formation of a doubly deprotonated [Ni(H₂L)] complex with the 12-membered ligand L⁵, as with the rest of the dioxotetra-amines, L⁶–L⁹. The stability of the L⁵ complex is assessed by the formation constant K_{NiH_2L} which is close to those for the open-chain homologues L⁹ and L¹¹, but is much smaller than those for the larger macrocycles L⁶–L⁸. This latter result may reflect the steric hindrance due to the unfolded (by double deprotonation) L⁵ ligand accommodating Ni²⁺ within the smallest ring cavity.

L⁵–L¹⁰, the longest-wavelength band (465 nm) was found for the L⁵ complex which may reflect the weakest Ni–N bond interactions, a fact supporting the anticipated steric constraint in the planar L⁵ complex.

In aqueous solutions of the dioxo-free macrocycles, the direction of equilibrium (19) varies with ring size;³ ratios of high-spin to low-spin forms at 25 °C are 99 : 1 (L¹), 13 : 87 (L²), 29 : 71 (L³), and 99 : 1 (L⁴). Complexes of L¹ and L⁴ are more than 99% in the blue form, while L² and L³ exist predominantly as the yellow form. As demonstrated by the equilibrium constants of equations (19) for L⁵–L⁸, the greater stability of the yellow form is due to the strong coplanarity resulting from incorporation of the two carbonyls. Especially remarkable are the complexes of the 12-membered L⁵

* The imide anion *N*-donors and the amine *N*-donors are postulated to have similar co-ordinative interactions and hence similar absorption characteristics. Supporting evidence in the literature includes an e.s.r. study of copper(II)–peptide complexes¹⁸ and a visible spectral study of copper(II)– and nickel(II)–peptide and homologous L¹⁰ complexes¹⁹ (cf. entries for L¹⁰ and L¹² in Table). In our study, the absorption maximum (450 nm) for the deprotonated L⁹ complex [Ni(H₂L)] is nearly the same as that (445 nm) for the dioxo-free (low-spin) 1,9-diamino-3,7-diazanonane complex [NiL]^{2+,2}

and the 15-membered L^8 ligands, where the spin states are reversed. The high-spin species with L^1 was considered as mixture of *cis* and *trans* octahedral forms.² It is unlikely that a minor (15%) component of the high-spin L^5 complex is in a *cis* geometry (due to the doubly deprotonated structure) and we consider a *trans* octahedral form which has two co-ordinated water molecules at the axial positions. The *trans* octahedral arrangement would certainly be responsible for the blue bands in the L^6 – L^8 complexes. Thermodynamic parameters for the blue-to-yellow conversion (19) with L^5 – L^8 were calculated by plots of $\ln K$ against T^{-1} . Interestingly, they are somewhat in a common range: ΔH 8.7 (L^5), 9.3 (L^6), 7.4 (L^7), and 7.1 kcal mol⁻¹ * (L^8), and ΔS 33 (L^5), 39 (L^6), 32 (L^7), and 35 cal K⁻¹ mol⁻¹ (L^8). The blue-to-yellow conversion is completely endothermic but this enthalpic disadvantage is more than compensated for by the entropy term. The entropy gain is due to the release of the co-ordinated water molecules. Our values for L^7 may be compared with those for the dioxo-free L^3 : ΔH 5.4 kcal mol⁻¹ and ΔS 20 cal K⁻¹ mol⁻¹.¹⁶ The greater entropy value with L^7 may indicate more complete liberation of the co-ordinated water molecules, which lends support to the theory that the dioxo-system has a stronger tendency to square-planar co-ordination.

Of the dioxo-free macrocycles L^1 – L^4 , the 12-membered L^1 forms the most exothermic bonds with low-spin Ni²⁺.² The two imide anions decrease the cavity of the 12-membered N_4 ligand thus making the 13-membered ring the size for the best fit. This notion is supported by the value of λ_{\max} for the L^6 complex which is the shortest of all those of the L^5 – L^8 complexes. However, adoption of a coplanar configuration to establish the strongest local interactions with Ni may require some strain of the ring conformation. Moreover, although the 14-membered ring encounters the least resistance to coplanarity, the coplanar N_4 cavity fits less well to the low-spin Ni²⁺ ion. Overall, the total balance puts L^6 just behind L^7 as regards their K_{NiH_2L} values. A similar argument was made for the interactions of L^2 and L^3 with low-spin Ni²⁺.³

Bossu and Margerum¹³ recently found that Ni³⁺, which is an uncommon oxidation state in aqueous solution, is stabilized by co-ordination with deprotonated peptide nitrogen atoms (such as in L^{11} or L^{12}). We have discovered a similar stabilization of Ni³⁺ by the dioxo-macrocyclic N_4 system in aqueous solutions containing Na₂[SO₄]. The electrochemical oxidation potentials E° determined by cyclic voltammetry are listed in the Table. Very recently,²⁰ a stable Ni³⁺– L^3 complex was reported, also electrochemically generated in acidic solutions in the presence of Na₂[SO₄]. We have repeated the experiment using our apparatus to obtain an E° value of 0.51 V (*vs.* s.c.e.) at pH 2.9, 25 °C, and I 0.5 mol dm⁻³ (Na₂[SO₄]). Our Ni³⁺–dioxo- N_4 species give rise to the distinct visible spectra of the trivalent oxidation state [*e.g.* 320–330 nm (L^5) or 310 nm (L^7)], like the peptides [327 nm (L^{12})]¹³ or the L^3 system (295

and 370 nm).²⁰ A thorough investigation of their chemistry is being conducted.

Apparently the ring size of the macrocycles affects the electrode potentials. The strength of the Ni²⁺–N in-plane interactions which explains the order of the E° values in the peptide complexes^{12,13} does not seem applicable to the present system. A fuller elucidation must await further studies, but our observation of the lowest E° value for L^5 is worthy of note. Conceivably the reduction of the cation size (from d^8 Ni²⁺ to d^7 Ni³⁺) may be most beneficial to the smallest planar macrocycle.

Copper(II)– L^5 Complexation.—Copper(II) also forms the [Cu(H₂L)] complex with L^5 at pH > 7. An extraordinary internal strain is presumed from the value of K_{CuH_2L} which is far smaller than for any other homologues in the Table. From the comparative values with other macrocycles the 12-membered ring strain is more pronounced in the copper(II) complex than in the nickel(II) complex. This is due to the longer Cu–N bond distances; *i.e.* the bigger Cu²⁺ ion is much more difficult to accommodate in the small cavity. The M–N distances in the saturated macrocyclic N_4 complexes lie in the range 2.03–2.10 Å for Cu²⁺ which is longer than 1.86–1.92 Å for low-spin Ni²⁺.³ The M–N bond lengths in the triply deprotonated peptide L^{12} complexes (four-N-co-ordinate) are also longer for Cu²⁺ (average 1.93 Å) than for Ni²⁺ (1.85 Å).^{4,5} The structure of the complexes is described as an extremely flattened tetrahedron for Cu²⁺, while it is truly square planar for Ni²⁺. With L^1 , Cu²⁺ adopts a square pyramid in which the conformation of L^1 is identical with that predicted for free L^1 ,³ and the internal strain is manifested in the d – d absorption at 600 nm.²¹ A similar complex geometry could be visualized for the doubly deprotonated L^5 , as judged from the similar d – d absorption. The relatively high absorption coefficient for the L^5 complex also indicates the effect of the local strain.

A significant increase in stability was predicted with the L^5 system on changing the metal ion from d^9 Cu²⁺ to d^8 Cu³⁺, due to the size contraction (to fit the hole) and the stronger preference for square-planar co-ordination by the d^8 system (similar to low-spin Ni²⁺, but slightly smaller due to the higher charge). As anticipated, we found the smallest E° value (0.42 V *vs.* s.c.e.) of all the dioxo-complexes investigated for Cu^{II}– L^5 . This value is in the range for the reported peptide complexes (*ca.* 0.4 V).¹² The Cu^{III}–dioxomacrocyclic N_4 complexes show characteristic yellow-to-brown visible absorptions at *ca.* 360 nm. Similar bands were reported for the complexes of the peptides L^{11} or L^{12} .¹² In preliminary studies we observed that while the Cu^{III}–peptide complexes and the Cu^{III}– L^9 complex are unstable (no sooner generated electrochemically than decomposed), the macrocyclic L^5 – L^8 complexes with Cu^{III} are in general more stable. Thus, our system may be suitable for studying copper(III) chemistry. Furthermore our study suggests that suitable choice of the ring size of dioxo-macrocycles can provide another model for biochemical oxidations. Recently,²² it was proposed

* Throughout this paper: 1 cal = 4.184 J.

that the monocopper enzyme, galactose oxidase, involves the copper(III) state in the oxidation of alcohols to aldehyde. We are currently investigating the model biochemical oxidations.

We thank Professor T. Fujisawa, Dr. T. Ogata, and Mr. K. Oikawa of Yamagata University for their help and suggestions regarding the construction of the potentiostat and potential scanner (used in the cyclic voltammetry).

[0/925 Received, 16th June, 1980]

REFERENCES

- ¹ M. F. Richardson and R. E. Sievers, *J. Am. Chem. Soc.*, 1972, **94**, 4134.
- ² L. Fabbri, *Inorg. Chem.*, 1977, **16**, 2667.
- ³ L. Fabbri, M. Micheloni, and P. Paoletti, *Inorg. Chem.*, 1980, **19**, 535.
- ⁴ H. C. Freeman and M. R. Tayler, *Acta Crystallogr.*, 1965, **18**, 939.
- ⁵ H. C. Freeman, J. M. Guss, and R.L. Sinclair, *Chem. Commun.*, 1968, 485.
- ⁶ M. Kodama and E. Kimura, *J. Chem. Soc., Dalton Trans.*, 1979, 325.
- ⁷ M. Kodama and E. Kimura, *J. Chem. Soc., Dalton Trans.*, 1979, 1783.
- ⁸ K. Ishizu, J. Hirai, M. Kodama, and E. Kimura, *Chem. Lett.*, 1979, 1045.
- ⁹ I. Tabushi, H. Okino, and Y. Kuroda, *Tetrahedron Lett.*, 1976, 4339; H. Kato, Doctoral Thesis, Department of Pharmaceutical Sciences, Kyushu University, 1977.
- ¹⁰ G. Schwarzenbach, 'Complexometric Titrations,' Interscience Publishers, New York, 1957.
- ¹¹ E. Itabashi and K. Oikawa, Annual Reports from the Research Institute for Science Education, Miyagi University of Education, 1972, **8**, 17.
- ¹² F. P. Bossu, K. L. Chellappa, and D. W. Margerum, *J. Am. Chem. Soc.*, 1977, **99**, 2195.
- ¹³ F. P. Bossu and D. W. Margerum, *J. Am. Chem. Soc.*, 1976, **98**, 4003; *Inorg. Chem.*, 1977, **16**, 1210.
- ¹⁴ P. Delahay, 'New Instrumental Methods in Electrochemistry,' Interscience Publishers, New York, 1954, p. 120; R. W. Murray and C. N. Reilley, 'Electroanalytical Principles,' Interscience Publishers, New York, 1963; E. R. Brown and R. F. Large in 'Techniques in Chemistry,' Part IIA, eds. A. Weissberger and B. Rossiter, Wiley-Interscience, New York, 1971, vol. 1, p. 440.
- ¹⁵ C. W. Davies, *J. Chem. Soc.*, 1951, 1256.
- ¹⁶ A. Anichini, L. Fabbri, P. Paoletti, and R. M. Clay, *Inorg. Chim. Acta*, 1977, **24**, L21.
- ¹⁷ L. Sabatini and L. Fabbri, *Inorg. Chem.*, 1979, **18**, 438.
- ¹⁸ D. C. Gould and H. S. Mason, *Biochemistry*, 1967, **6**, 801.
- ¹⁹ K. S. Bai and A. E. Martell, *J. Am. Chem. Soc.*, 1969, **91**, 4412.
- ²⁰ E. Zeigerson, G. Ginzburg, N. Schwartz, Z. Luz, and D. Meyerstein, *J. Chem. Soc., Chem. Commun.*, 1979, 241.
- ²¹ M. Kodama and E. Kimura, *J. Chem. Soc., Chem. Commun.*, 1975, 326.
- ²² A. Hamilton, P. K. Adolf, J. de Jersey, G. C. Dubois, G. R. Dyrkacz, and R. D. Libby, *J. Am. Chem. Soc.*, 1978, **100**, 1899.